Ab initio molecular dynamics simulations of SO 2 solvation in choline chloride/glycerol deep eutectic solvent

Alexander Korotkevich, Dzmitry S. Firaha, Agilio A.H. Padua, Barbara Kirchner

Ab initio molecular dynamics simulations of SO_2 solvation in choline chloride/glycerol deep eutectic solvent

Alexander Korotkevich [a, b], Dzmitry S. Firaha [a, d, **], Agilio A.H. Padua [c], Barbara Kirchner [a, *]

[a] Mulliken Center for Theoretical Chemistry, University of Bonn, Beringstr. 4+6, D-53115 Bonn, Germany
[b] Chemistry Department, Lomonosov Moscow State University, 1-3 Leninskiye Gory, GSP-1, Moscow, 119991, Russia
[c] Institute of Chemistry of Clermont-Ferrand, Universit´e Blaise Pascal & CNRS, 24 Avenue Blaise Pascal, 63178 Aubiere, France [d] AICES Graduate School, RWTH Aachen University, Schinkelstr. 2a, D-52056 Aachen, Germany

Deep eutectic solvents (DESs) are mixtures of ionic compounds and molecular hydrogen bond donors. Due to the many components and their different interacting subgroups, they give rise to a plethora of many different interactions which can be studied by ab initio molecular dynamics simulations, because within this method all the forces are calculated on the fly and no parametrization prior to the calculation is necessary. Since DESs can be applied in gas capture, for example for SO_2 absorption, we performed ab initio molecular dynamics studies of both the pure choline chloride/glycerol DES and the same mixed with SO_2. We identified the hydrogen bonding and other specific interactions between all components. With addition of SO_2, we observed a decrease in the anion-OH group interplay, because the chloride anions form complexes with the SO_2 molecules. Furthermore, the SO_2 molecules are incorporated into the hydrophobic network and the interaction between the hydrogen bonds of all OH groups remain constant. This decrease of anion-OH interaction might be responsible for the more fluid state of the SO_2-DESs mixture than the pure DES.

1. Introduction

Sulfur dioxide (SO_2) which is emitted to the atmosphere as a byproduct of the combustion of fossil fuels is becoming one of the major air pollutants. This gas together with nitrogen oxides causes acid rains and harms humans health, animals, and plants. Anthropogenic SO_2 emissions are ten times larger than emissions from natural volcanic activity [1,2] and this creates a worldwide ecological problem.

Nowadays around 90% of industrially emitted SO_2 is captured by limestone technique [3,4]. The main shortcomings of this process are the irreversibility and high water consumption. Additionally, the byproducts of the limestone processes are low valued gypsum and undesirable carbon dioxide [5]. The development of modern technologies is of high importance in order to change the common desulfurization technique and improve the current situation. The novel approaches involving absorption and chemical transformation of SO_2 were described in several publications during the past decade [3,6–8]. Application of ionic liquids [9–12] (ILs) for SO_2 capture is one of the most promising alternatives to conventional absorption technology. The compounds of this class are entirely composed of ions and some of them possess useful properties such as low vapor pressure and high thermal stability in contrast to typical organic solvents [13]. Notably, gas absorption [14] in ILs is reversible [15], it does not demand water, and it creates no byproducts [16]. Moreover, various methods of organic chemistry allow tuning the structure of cations and anions to gain desirable properties, such as high SO_2 absorption capacity [17–20]. However, the pure biodegradability and toxicity of ILs have to be taken into account [21–23]. A preparation protocol requires additional solvents and may invoke time-consuming purification (e.g. vacuum drying or column chromatography) that makes ILs quite expensive chemicals as well [16,24].

During the past decade, another type of solvents related to ILs,

* Corresponding author. Tel.: +49 0 228 73 60442.
** Corresponding author. Mulliken Center for Theoretical Chemistry, University of Bonn, Beringstr. 4+6, D-53115 Bonn, Germany. Tel.: +49 0 241 80 99755.
E-mail addresses: d.s.firaha@gmail.com (D.S. Firaha), kirchner@thch.uni-bonn.de (B. Kirchner).

namely deep eutectic solvents (DESs), has become an object of high interest [25–28]. A DES is a mixture of ionic compounds (usually organic) and hydrogen bond donors. Such a mixture has a melting point much lower than the melting points of the isolated compounds [25]. Usually, tertiary ammonium or phosphonium salts are employed as ionic species. For example, choline chloride (2-hydroxy-N,N,N-trimethylethanaminium chloride, [Ch][Cl]) became very popular due to its commercial availability and biocompatibility. The commonly applied hydrogen bond donors include polar organic compounds, such as polyols, carboxylic acids, urea, and thiourea derivatives [26]. Interestingly, some physical properties of DESs are close to those of ILs [25–28]. However, the essential advantage of DESs is their better environmental biocompatibility and lower toxicity compared to traditional ILs [29–32]. Another significant advantage of DESs is their low price due to the presence of the available starting materials and a simple preparation protocol. This protocol includes only mixing of two or more compounds and gentle heating of the mixture. Thus, DESs might be considered as an example of a cheap alternative "green" media for various processes including SO_2 absorption [25–28,33].

Experimental investigation of SO_2 absorption by DESs was conducted in several studies. Inorganic thiocyanates based DESs [34], as well as organic betaine based DESs were tested as SO_2 [35] absorbents and moderate capacity up to 2 mol(SO_2)/mol(DES) was shown. Eutectic mixtures of choline chloride [36] and glycerol [37], urea, thiourea, malonic acid, ethylene glycol [38], levulinic acid [39] efficiently absorb SO_2: capacities vary from 1.4 to 3 mol(SO_2)/mol(DES) at 298 K. Average capacities for DESs described are comparable with typical data for ILs. Furthermore, absorption is reversible in all cases: desorption is reached by bubbling of nitrogen at 323 K through the mixture of DES and SO_2. No significant absorption capacity decrease is observed after five consecutive absorption-desorption cycles, which makes DESs promising objects for industrial applications.

Experimental and theoretical research was conducted to reveal the underlying types of interactions in DES and DES+SO_2 systems. The internal structure of DESs was studied employing infra-red spectroscopy, density functional theory (DFT)-calculations, and molecular dynamics (MD) simulations [40–47]. The plethora of hydrogen bonds is observed in all cases and considered to be responsible for DESs behavior. Furthermore, the complex structure of cations and hydrogen bond donors causes the formation of various intermolecular aggregates with the anion and the potential energy surface contains lots of nearby minima, which leads to the high mobility of anions in the DESs media and low melting point.

Only a few studies to establish SO_2 absorption mechanisms were carried out. The data presented in Refs. [37,38] gives rise to a hypothesis of physical absorption of sulfur dioxide caused by charge transfer from the anion to the sulfur atom of SO_2. This hypothesis was confirmed later by DFT study combined with explicit solvation model [48]. However, a detailed description of this mechanism is still missing.

The [Ch][Cl]/glycerol deep eutectic solvent is a typical example and was reported as a promising SO_2 absorbent [37]. In our previous studies of SO_2 absorption [49] by ILs ab initio molecular dynamics (AIMD) [50] simulations were used as a powerful instrument in the theoretical description of liquid systems. In AIMD the forces are calculated on the fly, which means that no preparametrization of any force field is necessary. In addition, AIMD considers many-body effects and thus polarizability is directly included, which is in standard classical simulations neglected. The recent developments of polarizeable force fields for ILs appear to be a promising solution for this problem [51–55]. The drawbacks of AIMD are small system sizes and short simulation times. However, this outweighs largely the fact that standard simulations might not be able to resolve the specific interactions this precisely, especially when considering how many components – and thus mixed interactions — are present. To the best of our knowledge, no data of AIMD-studies of these systems and gas absorption by DESs whatsoever were reported until now.

2. Systems investigated

In order to understand how SO_2 is dissolved in the choline chloride/glycerol deep eutectic solvent (DES) and to investigate the influence of the DES onto the solute SO_2 and vice versa as well as to understand the solvation modes, we simulated two systems. Namely, the pure DES and the DES mixed with the experimental saturated amount of SO_2. The molecular picture of the systems under study as well as the labeling for each molecule are presented in Fig. 1. In the following analysis we will always refer to this labeling to allow for an easier understanding of the different graphs.

In the first system, denoted **DES**, 32 glycerol molecules, Glc, were simulated with 32 ion pairs of choline chloride, [Ch][Cl]. For the second system, denoted **DES+SO_2**, 80 SO_2 molecules were added to the first system. The number of SO_2 molecules corresponds to the 2.5:1:1 (SO_2:Glc:[Ch][Cl]) ratio. The chosen composition corresponds the experimental absorption data at 20 °C [37].

3. Computational details

Starting geometries for ab initio molecular dynamic (AIMD) simulations were prepared from a classical molecular dynamic simulation utilizing OPLS (Optimized Potentials for Liquid Simulations) force field and RESP (Restrained Electrostatic Potential) charges with the aid of large-scale atomic/molecular massively parallel simulation (LAMMPS) package [56]. For the first system, a

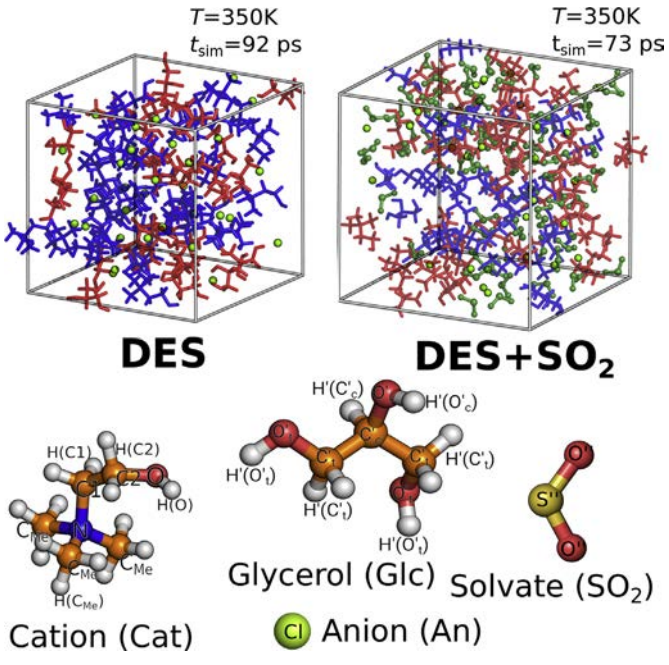

Fig. 1. Above: Representation of simulation boxes. Left: **DES** consisting of 32 ion pairs of choline (cation) chloride (anion) and 32 glycerol molecules; Right: **DES** and 80 molecules of sulfur dioxide (**DES+SO_2**). Color code: cations in blue; anions in light-green; glycerol in red and SO_2 in dark green. Below: ball-and-stick representation of molecules. Please note, atoms of the cation and anion are marked without primes, atoms of glycerol with one prime, and, atoms of the sulfur dioxide with two primes. (For interpretation of the references to colour in this figure legend, the reader is referred to the web version of this article.)

cluster of two Glc molecules and two [Ch][Cl] ion pairs was used to prepare a cubic box with 32 Glc and 32 [Ch][Cl] species. For the second system, five SO_2 molecules were added to the existing cluster to obtain a cubic box with 32 Glc, 32 [Ch][Cl], and 80 SO_2 species. An edge length was set up to 2217.8 pm for the first system in order to reproduce the density at 350 K interpolated from experimental data between 298.15 and 368.15 K [57]. For the second system, the box length was set up to 2609.5 pm to reproduce the density obtained assuming an ideal mixing of DES and SO_2 at 350 K. The density of liquid SO_2 was taken from a database of Thermophysical Properties of Fluid Systems (http://webbook.nist.gov/chemistry/fluid/) for saturated conditions at 350 K.

AIMD simulations were carried out with density functional theory (DFT) within the CP2K [58] program package using the QUICKSTEP module [59]. Here, the hybrid Gaussian and plane waves (GPW) approach is used to calculate the energies and forces on the atoms. The molecularly optimized double-ζ basis set (MOLOPT-DZVP-SR-GTH) [60] was applied to all atoms together with the generalized gradient approximation (GGA) utilizing the Becke–Lee–Yang–Parr (BLYP) [61,62] functional and the corresponding BLYP Goedecker–Teter–Hutter (GTH) pseudopotentials for core electrons [63–65]. A 280 Ry density CUTOFF criterion with the finest grid level was employed together with multigrid number 5 (NGRID 5 and REL_CUTOFF 40) using the smoothing for the electron density (NN10_SMOOTH) and its derivative (NN10) [59]. The deficiency of the dispersion interactions for the GGA functional was corrected using empirical dispersion correction (D3) scheme with Becke–Johnson damping [66,67]. Several times it was shown by our group as well as by others that this correction is important for systems of similar complexity to ionic liquids [11,11,68–75] or water [76]. For the self-consistent field (SCF) calculation, the default value (1.0E-5) was used as target accuracy for the SCF convergence. The direct inversion of the iterative subspace (DIIS) minimizer [58] was used to reach a faster orbital transformation. The maximum number of SCF iterations to be performed for one iteration was set to 200 while a maximum of 10 iterations was performed for outer SCF loops.

In order to observe and analyze the temporal development of the systems over time, AIMD simulations were carried out applying periodic boundary conditions in order to avoid boundary effects. The simulation boxes for both systems were equilibrated for 3.0 ps using canonical (NVT) ensemble with the Nosé–Hoover-chain thermostats [77,78] for individual atoms with a time constant of 100 fs and with a time step of 0.5 fs. The temperature for equilibration was set to 450 K in order to increase the sampling. For the following production runs, the temperature was set up to 350 K. The production simulations were run for 94.1 and 74.7 ps for the first and the second system, respectively. The time constant and the time step were kept the same as for the equilibration.

Our open source program TRAVIS (Trajectory Analyzer and Visualizer) was used to examine the simulated systems [79]. This powerful tool enables the time-dependent investigation of structural features of the solvent and the solute, intra- and intermolecular interactions within or between the components and the elucidation of chemical reaction mechanisms by calculating different distribution functions between relevant atoms and positions of the observed systems. The most used features are radial distribution functions (RDFs) and distance distribution functions, which are visualized with the aid of the program gnuplot (version 5.0) [80] for the generation of two- and three-dimensional plots of functions, data, and data fits or with the xm-grace software [81]. Furthermore, we applied the recently developed Voronoi analysis to decompose the system into different subgroups [82,83].

4. Results

4.1. Conformational analysis

Before analyzing the plethora of hydrogen bonds that are possible in the **DES** or that are possibly perturbed by the solvate, we consider the conformational flexibility of the cation and the glycerol molecule, because depending on them, different hydrogen bonds will be possible. The corresponding conformational analyses are given in Fig. 2. On the left side, we show the behavior of the cation. Clearly, a domination of gauche conformers for the cation can be noticed in the pure **DES**. Upon SO_2 addition this preference of the gauche conformer becomes even more extreme, namely the average number of molecules in gauche conformation becomes larger. On the right side of Fig. 2, the distance distribution of glycerol is presented. Of course, due to the molecular structure, four different conformations are possible. While the conformers with O'_t-O'_t distance of ≈275 pm and ≈350 pm are only weakly populated, in both, the **DES** and the **DES**+**SO_2** systems, the two other conformers are highly populated. These are a gauche-trans and gauche-gauche conformer with an obvious domination of gauche-trans form. An influence of the SO_2 molecules is also apparent, the gauche-gauche conformation becomes more important and all peaks are shifted to larger distances. Thus, upon SO_2 addition the cation seems to assume more compact conformers while the alcohol seems to populate larger distances and more of the gauche-gauche conformer which separates within the molecule the polar from the non-polar groups.

4.2. Structure of hydrogen bonds with the anion

Fig. 3 presents the RDFs for each possible anion-hydrogen atom interaction. Obviously, the strongest hydrogen bonds are between the chloride and the OH groups of the cation and the alcohol. Interestingly, the alcohol shows higher peaks than the cation which indicates the importance of the glycerol-anion interaction. This was observed before in a 1:1 mixture of oxalic acid and choline chloride by Zahn and coworkers [46]. The observed order is as follows $O'_c > O'_t \approx O$. The remaining hydrogen bonds which are donated by carbon atoms are weaker or less often occurring and show an order as follows $C1 \approx C_{Me} > C'_c > C2 > C'_t$. In the presence of SO_2 molecules, the **DES** system changes the concentration because it becomes diluted by a fourth compound which renders the direct comparison of peak heights between the **DES** and **DES**+**SO_2** systems difficult, since the RDFs are calculated with respect to the average density. Thus when diluting a system naturally the peaks must be increasing. However, there is one very striking common feature, namely all hydrogen bond peaks decrease, thus, the hydrogen bonds are weaker or less often occurring when the solute is presented. Within this general decrease also the order changes with the most prominent example being the Cl⋯ H-O'_c hydrogen bond, also there is the complete disappearance of the weak Cl⋯H-C'_c hydrogen bond, see Fig. 3. Considering the integrated RDFs multiplied by the density instead allows for the comparison of the **DES** and **DES**+**SO_2** systems.

From Table 1 it is obvious that the effects are much more extreme than anticipated from the RDF peak heights. The reduction of the coordination for example for the H′(O′c)-Cl hydrogen bond is more than 3 times instead of only about 2.5 times as indicated by the peak heights of the RDF.

4.3. Interaction of the solute

The RDFs reflecting the interactions of the sulfur atoms with the anion and the oxygen atoms of other sulfur dioxide molecules are

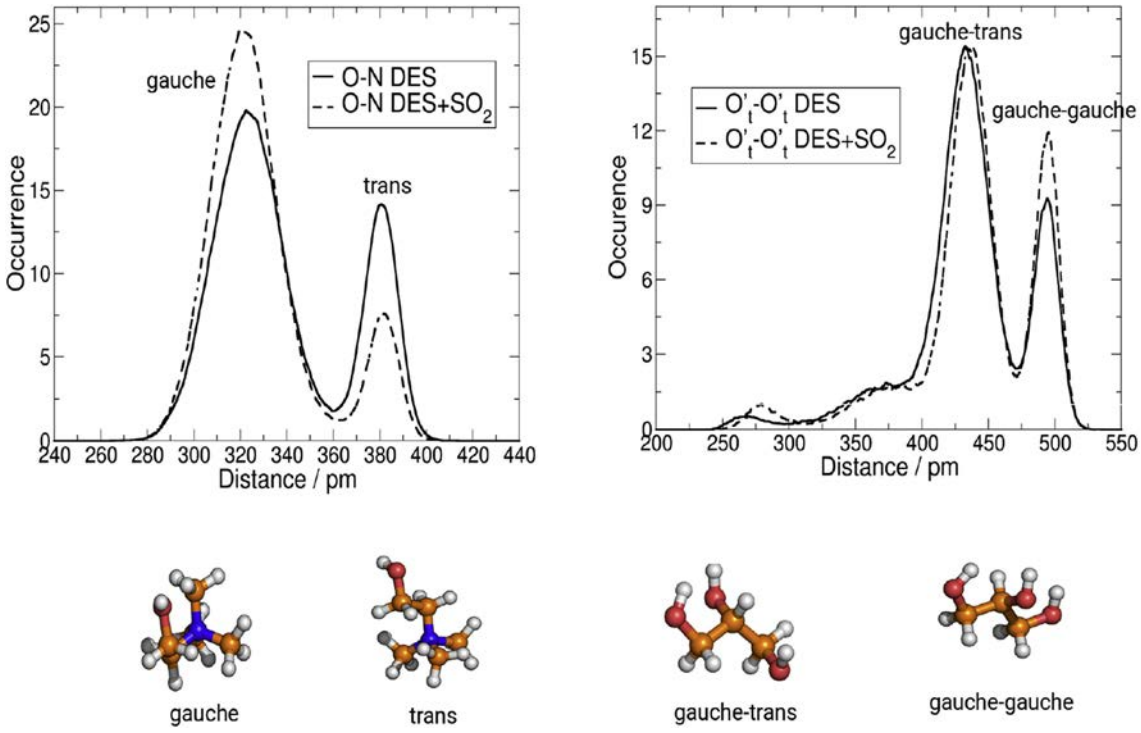

Fig. 2. Conformational analysis of the cation and glycerol. The distance distribution functions show the occurrence plotted against the specific distances given in the legend which reflects the conformation. Solid lines: pure DES; Dashed lines: DES mixed with SO_2.

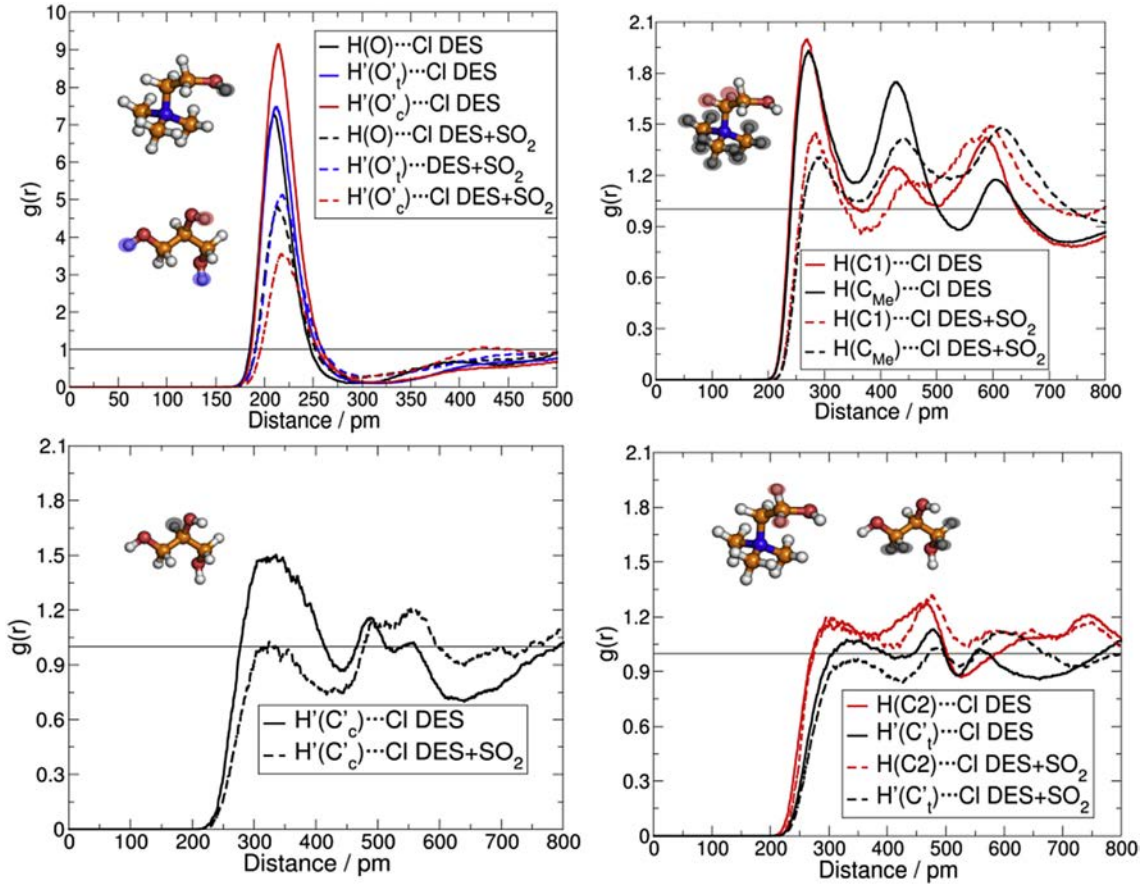

Fig. 3. RDF of anion-hydrogen atom interactions. For each curve the interacting hydrogen atoms are labeled with a transparent ellipse that is colored according to the corresponding curve. (For interpretation of the references to colour in this figure legend, the reader is referred to the web version of this article.)

Table 1
Coordination number by integration of the first RDF peak of functions shown in Fig. 3 multiplied by the density and $4\pi r^2$.

RDF	DES	DES+SO_2
H(O)-Cl	0.50	0.23
H′(O_t')-Cl	1.11	0.56
H′(O_c')-Cl	0.68	0.20

presented in the Fig. 4. The SO_2-Cl RDF exhibits a very pronounced peak.

There is also an intermolecular S″-S″ interaction, but this is weaker than the S″-Cl interplay. However, it is similar albeit a bit higher to the one obtained by Ribeiro [85] for liquid sulfur dioxide suggesting a liquid-like state of SO_2 within the **DES**. Furthermore, the double peak is presented indicating that the minimum structure (see Table 2 and also suggested by Ribeiro) is populated in our mixture as well as structure **C** or **D**, see Fig. 4 right hand side.

The observed weakening of the anion hydrogen bonds shown in Fig. 3 in the presence of the SO_2 molecules and the strong Cl-SO_2 might be correlated. Both types of interactions (the Cl-SO_2 and the weaker SO_2-SO_2) may be responsible for the favorable SO_2 absorption in **DES**. A possible scenario is the incorporation of the SO_2 molecules into the hydrogen bond network of the **DES**. In order to explore this, the RDFs of the SO_2 oxygen atoms (O″) with the acidic hydrogen atoms is shown in Fig. 5.

Obviously, there are no hydrogen bonds or stronger interplays between the hydrogen atoms donated by the oxgens and the SO_2 molecules. Thus, SO_2 is not incorporated into the hydrogen bond network, but rather perturbs it and forms strong associates with the chloride anion.

4.4. OH-hydrogen bond network

In order to understand these changes further, we consider in Fig. 6 the hydrogen bonds between all possible polar OH group combinations of the cations and the glycerol molecules. All first peak heights in the **DES** system are below 2.8 while the ones for the OH groups with the anion show values between 7 and 9 (see Fig. 3), indicating a much more preference for the OH-anion interaction. Nevertheless, these interactions seem to be present and thus relevant. Turning to the **DES**+**SO_2** system the peak height for both

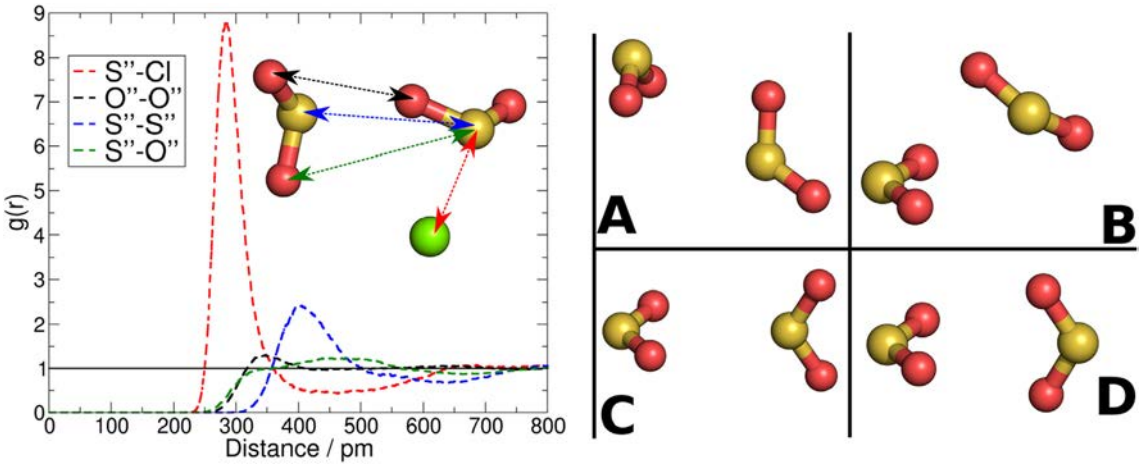

Fig. 4. RDFs illustrating the solvate-anion and solute-solute interactions. Shown is the chloride-sulfur atom function in red with dashed lines and the oxygen-sulfur atom function in green with dashed lines, The sulfur-sulfur function is marked blue and the O″-O″-RDF is marked green. Integration of the red curves from 0 to 400 pm gives 1.05. Below we show four quantum chemically (B3LYP/def2-TZVP (D3 [66], m5, scfconv = 8)) optimized structures obtained by the turbomole suits [84]. (For interpretation of the references to colour in this figure legend, the reader is referred to the web version of this article.)

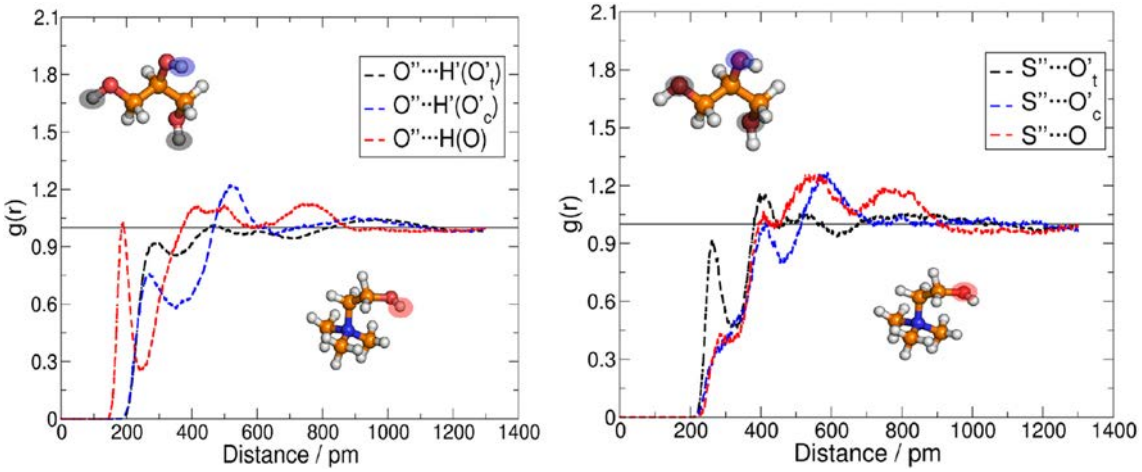

Fig. 5. RDFs illustrating the solvate-hydrogen atom and solvate-oxygen atom interactions. Shown is the hydrogen-oxygen(SO_2) atom function and the oxygen-sulfur (SO_2) atom function with dashed lines.

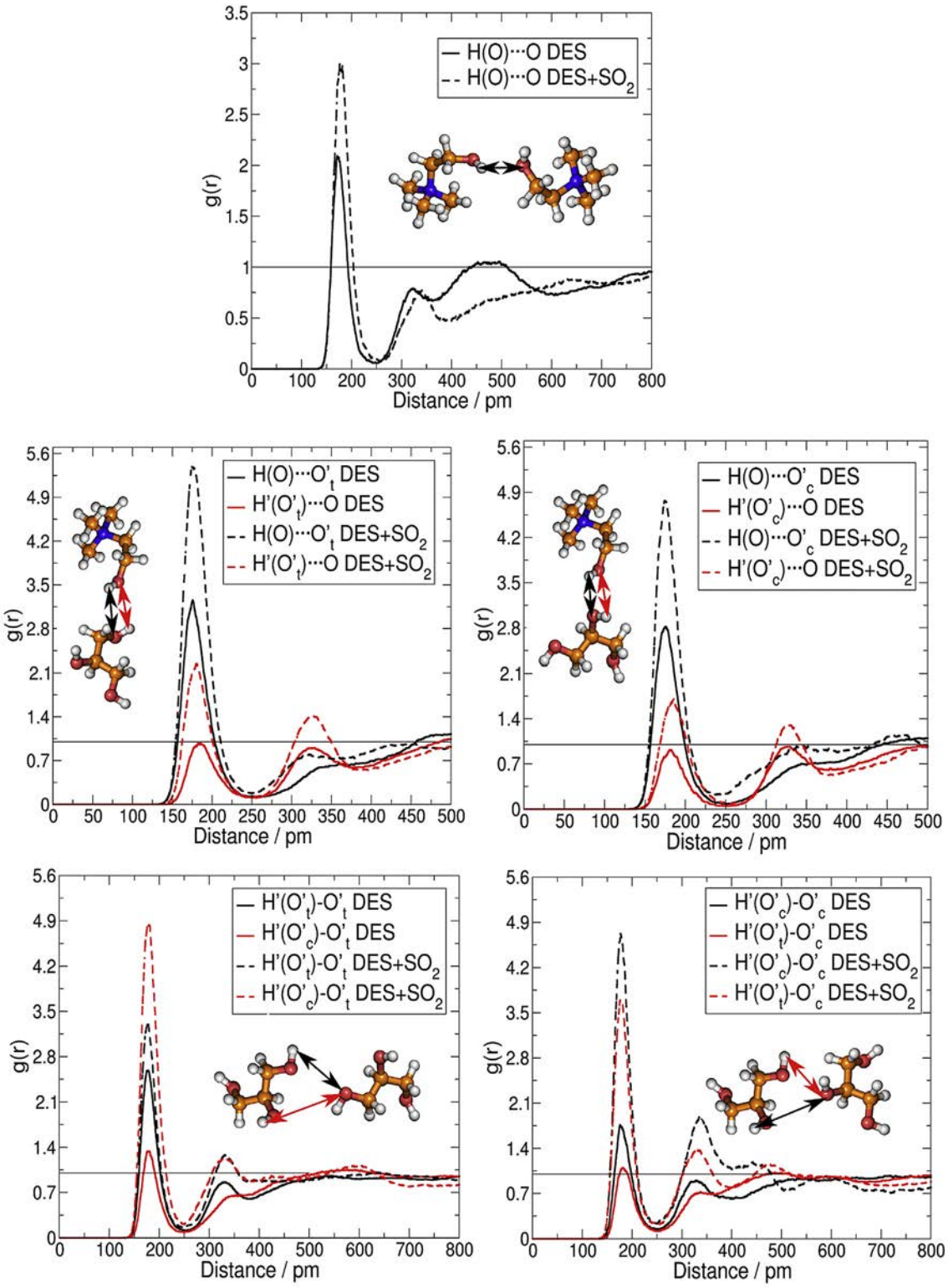

Fig. 6. RDFs illustrating the hydrogen atom and oxygen atom interactions of the cation and glycerol themselves and with each other. Solid lines: pure **DES**; Dashed lines: **DES**+**SO_2**.

the OH-OH and the OH-anion interaction occur around 3—5. Thus, showing that the importance of interaction was shifted to the OH-OH from the one between OH and the anion.

According to the more diluted system, in all possible O···H combinations the first maximum of the corresponding RDF increases in the presence of the SO_2 molecules. In order to allow the concentration independent comparison, we show in Tables 1 and 3 the coordination numbers. With the exception of the $H'(O'_t)$-O'_t and the H(O)-O'_c combination all hydrogen bond coordination numbers increase slightly or stay in the same range.

Table 2
Results of quantum chemical calculations: E_{rel} relative energy and E_{adia} adiabatic binding energy in kJ/mol as well as distances in pm. Please note, in the last line for the SO_2-Cl adduct no relative energy is given and the r(S″-Cl) distance in pm.

No	E_{rel}	E_{adia}	r(S″-S″)
A	0.0	−14.9	381.4
B	1.0	−13.9	389.4
C	5.2	−9.7	403.6
D	5.6	−9.3	414.0
SO_2-Cl		−63.4	317.8

Table 3
Coordination number by integration of the first RDF peak of functions shown in Fig. 6 multiplied by the density and $4\pi r^2$.

RDF	DES	DES+SO_2	RDF	DES	DES+SO_2
H(O)-O	0.09	0.09	–	–	–
H′(O'_t)-O'_t	0.53	0.41	H′(O'_c)-O'_c	0.10	0.16
H′(O'_c)-O'_t	0.15	0.31	H′(O'_t)-O'_c	0.14	0.24
H(O)-O'_t	0.26	0.32	H(O)-O'_c	0.16	0.13
H′(O'_t)-O	0.12	0.14	H′(O'_c)-O	0.05	0.06

The emerging picture is that, while SO_2 is captured by the **DES**, it competes with the cation and the glycerol molecules for the interaction with anion. Thus, it suppresses the hydrogen bonds of cation with anion and of glycerol with the anion. At the same time the OH-OH cation-cation, cation-glycerol and glycerol-glycerol interplays become slightly more probable.

4.5. Weak interactions

A large part of the solvation structure is determined also by the apolar moieties of the molecules. In Fig. 7 left panel we show the probability of the carbon atom-carbon atom distances for the cation-cation, cation-glycerol and glycerol-glycerol combinations. While the cation-cation interplay is negligible, the cation-glycerol and even more so the glycerol-glycerol function seems to be more important. Upon SO_2 addition the glycerol-glycerol peak increases which is a pure diluting effect, i.e. the coordination number decreases from 41.8 to 27.1. The other peaks all decrease which shows that these interactions loose even more importance when the SO_2 is present. This goes along together with a sizable interplay between the SO_2 oxygen atoms and the cation as well as glycerol (although to a lesser extent), see Fig. 7 right panel. Both interactions are comparable to the interplay of the SO_2 with itself which suggests that there is a network of dispersion-like interaction ranging from the SO_2 molecules to the nonpolar parts of the cations and the glycerol molecules.

4.6. Domain analysis

The domain analysis which is based on the radical Voronoi tessellation and which helps to detect clustering and neighborhood relation in the bulk was recently introduced [83] and applied [86] by us and is freely available in TRAVIS [79]. Within this domain analysis it is possible to define different subsets (even within molecules) and determine there relation with each other and the other subsets. Table 4 and Table 5 contain the domain analysis for the pure **DES** and the **DES**+**SO_2** respectively. We defined the following subset:

1 Polar: all OH group (of all molecules)
2 Nonpolar: all CH group (of all molecules)
3 Anion: anions
4 SO_2: sulfur dioxide molecules, which we also decomposed into a S″and a O″ subset.

Due to the chemical bonding between CH and OH groups, there is a lot of surface area shared between the two of them. Comparing the two Tables 4 and 5 it is obvious, that the Polar-Polar interplay increases slightly, upon SO_2 addition. This was observed already in Fig. 6. However, the Polar groups are not in one domain but they are dispersed within the system which increases when the SO_2 is present. The Anion-Polar contact is decreased largely with sulfur dioxide and interestingly, so is the shared surface area of the Nonpolar-Nonpolar subsets. Nevertheless, the Nonpolar subsets still remain in one domain only, i.e. they must be all somewhat interconnected.

Table 4
Domain analysis for **DES**. First column: Reference subset; columns 2–4 give the contact area and in parenthesis the neighbor count. Last column lists the domain count abbreviated dc. Polar = OH groups, Nonpolar = CH-groups, Anion = A.

Ref. subset	Polar	Nonpolar	Anion	dc
Polar	8.9(3.3)	29.9(5.3)	4.2(1.0)	4.1
Nonpolar	119.4(21.2)	102.7(15.4)	37.5(6.4)	1.0
Anion	16.7(3.8)	37.5(6.4)	0.1(0.4)	28.3

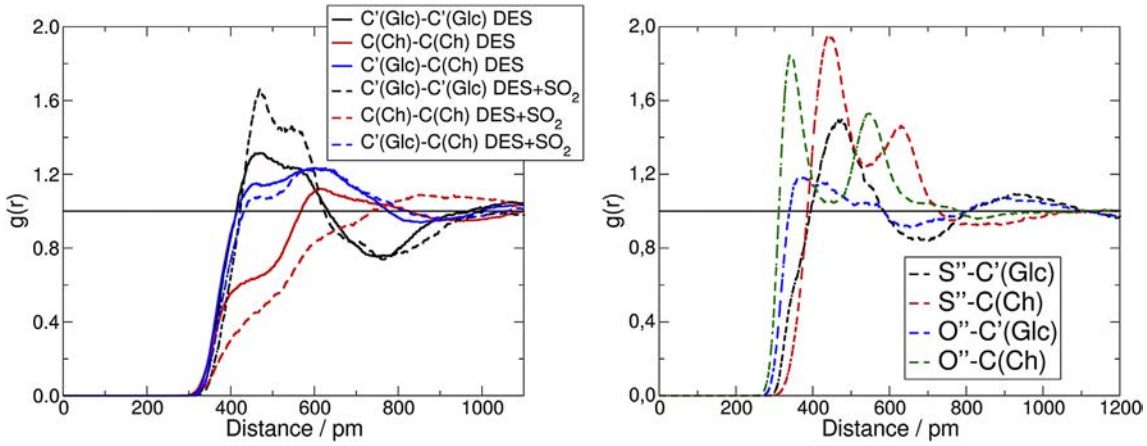

Fig. 7. RDF of weak interaction. Left panel: RDF of carbon atom-carbon atom from the cation and the glycerol. Right panel: RDF of SO_2 with cation and alcohol.

Table 5
Domain analysis for **DES**+**SO_2**. First column: reference subset, columns 2–7 give the contact area and in parenthesis the neighbor count. Last column lists the domain count abbreviated dc. Polar = OH groups, Nonpolar = CH-groups, Anion = A.

Ref.	Polar	Nonpolar	Anion	SO_2	S″	O″	dc
Polar	9.8(2.9)	26.2(3.8)	2.1(0.5)	7.8(2.3)	2.7(1.2)	5.1(2.4)	9.6
Nonpolar	104.8(15.2)	60.1(10.8)	21.3(4.0)	117.8(14.5)	21.7(9.6)	96.0(17.5)	1.0
Anion	8.4(2.1)	21.3(4.0)	0.1(0.1)	26.8(3.7)	20.2(3.1)	6.7(5.4)	29.9
SO_2	12.5(3.6)	47.1(5.8)	10.7(1.5)	24.7(4.4)	–	–	1.05
S″	4.4(1.9)	8.7(3.8)	8.1(1.2)	–	2.2(1.8)	29.6(4.7)	17.9
O″	4.1(1.9)	19.2(3.5)	1.3(1.1)	–	14.8(2.3)	5.5(3.6)	1.9

5. Conclusion

In this work, we investigated the pure deep eutectic solvent (DES) choline chloride/glycerol and SO_2 dissolved in the choline chloride/glycerol liquid from ab initio molecular dynamics simulations (AIMD). In AIMD the forces are calculated on the fly which means that no pre-parametrization of any force field is necessary. In addition, AIMD considers many-body effects and thus polarizability is directly treated.

We analyzed the system with respect to structural aspects, especially we considered the changes in hydrogen bonding and the specific solvation in order to gain an understanding of the SO_2 solvation process.

We observe by radial distribution functions, and integration of their first peaks to obtain coordination numbers, strong hydrogen bonding of the OH groups — in particular of the glycerol — with the chloride anion. There is also hydrogen bonding of the OH groups between all combinations of the choline cation and glycerol. However, these bonds seem to be less strong than the ones with the anion. Interplay between the C-H groups and the anion is also apparent in some cases, especially between the cation and the anion. Considering the interactions between the C-H groups only, the major contributions to this dispersion-like interaction comes from the glycerol-glycerol and glycerol-cation combination.

Per domain analysis the above listed observations are confirmed. In contrast to ionic liquids, the polar groups do not form a single domain, but there are a few interrupted islands which might be due to the fact that in this study we collected the anions in a separate subset. Interestingly, the nonpolar groups form one domain and the anions are dispersed in the system.

For the design of further DES, it will be interesting to choose different components such as more or less basic anions in combination with shorter and longer nonpolar groups in order to counterbalance the hydrogen bonding network effects.

Comparing these results to the SO_2-diluted system, we observe a strong interaction between the anion and the SO_2. SO_2 and the OH groups do not show strong spatial correlations, but SO_2 molecules among themselves and with the nonpolar CH groups show sizable first RDF peaks and coordination numbers. All this accompanies a disruption of the anion-OH network to a third of its original constitution. The nonpolar-nonpolar network is also disturbed in that the SO_2 now participates in it. The OH network increases only a bit, and almost maintains its original structure.

All the above listed results lead to the following emerging picture: The chloride anions bind to the SO_2 molecules inside the liquids. One might speculate that once enough SO_2 is absorbed, it behaves like liquid SO_2. It was shown by Ribeiro [85] that liquid SO_2 is very Lennard-Jones-like. Thus, it also interacts with the hydrophobic part of the liquid which might be another reason for the good absorption. In future studies this has to be put onto solid ground by for example varying the nonpolar part, i.e., applying larger side chain and investigating their effect on the SO_2 absorption. However, one might have to be careful that a sizeable desorption will be still possible.

Another important point is that, upon SO_2 absorption, the liquid becomes more fluid. This may be attributed to the disrupted anion-OH group network which we observed in our AIMD simulations.

Appendix A. Supplementary data

Supplementary data related to this article can be found at http://dx.doi.org/10.1016/j.fluid.2017.03.024.

References

[1] P.J. Wallace, Volcanic SO_2 emissions and the abundance and distribution of exsolved gas in magma bodies, J. Volcanol. Geotherm. Res. 108 (2001) 85–106.
[2] S.J. Smith, J. van Aardenne, Z. Klimont, R.J. Andres, A. Volke, S. Delgado Arias, Anthropogenic sulfur dioxide emissions: 1850–2005, Atmos. Chem. Phys. 11 (2011) 1101–1116.
[3] C. Wang, H. Liu, X.-Z. Li, J. Shi, G. Ouyang, M. Peng, C. Jiang, H. Cui, A new concept of desulfurization: the electrochemically driven and green conversion of SO_2 to $NaHSO_4$ in aqueous solution, Environ. Sci. Technol. 42 (2008) 8585–8590.
[4] X. Ma, T. Kaneko, T. Tashimo, T. Yoshida, K. Kato, Use of limestone for SO_2 removal from flue gas in the semidry FGD process with a powder-particle spouted bed, Chem. Eng. Sci. 55 (2000) 4643–4652.
[5] N.H. Stern, H.M. Treasury, et al., Stern Review: the Economics of Climate Change, vol. 30, HM treasury London, 2006.
[6] L. Philip, M.A. Deshusses, Sulfur dioxide treatment from flue gases using a biotrickling FilterBioreactor system, Environ. Sci. Technol. 37 (2003) 1978–1982.
[7] Y. Zhi, Y. Zhou, W. Su, Y. Sun, L. Zhou, Selective adsorption of SO_2 from flue gas on triethanolamine-modified large pore SBA-15, Ind. Eng. Chem. Res. 50 (2011) 8698–8702.
[8] X. Li, L. Zhang, Y. Zheng, C. Zheng, SO_2 absorption performance enhancement by ionic liquid supported on mesoporous molecular sieve, Energy Fuels 29 (2015) 942–953.
[9] T. Welton, Room-temperature ionic liquids. solvents for synthesis and catalysis, Chem. Rev. 99 (1999) 2071–2084.
[10] T. Welton, Ionic liquids in catalysis, Coord. Chem. Rev. 248 (2004) 2459–2477.
[11] B. Kirchner, O. Hollóczki, J.N. Canongia Lopes, A.A.H. Pádua, Multiresolution calculation of ionic liquids, WIREs Comp. Mol. Sci. 5 (2014) 202–214.
[12] B. McLean, H. Li, R. Stefanovic, R.J. Wood, G.B. Webber, K. Ueno, M. Watanabe, G.G. Warr, A. Page, R. Atkin, Nanostructure of [Li(G4)] TFSI and [Li(G4)] NO_3 solvate ionic liquids at HOPG and Au(111) electrode interfaces as a function of potential, Phys. Chem. Chem. Phys. 17 (2015) 325–333.
[13] S. Tian, Y. Hou, W. Wu, S. Ren, C. Zhang, Absorption of SO_2 by thermal-stable functional ionic liquids with lactate anion, RSC Adv. 3 (2013) 3572–3577.
[14] D. Almantariotis, A.S. Pensado, H.Q.N. Gunaratne, C. Hardacre, A.A.H. Pádua, J.-Y. Coxam, M.F. Costa Gomes, Influence of fluorination on the solubilities of carbon dioxide, ethane, and nitrogen in 1-n-fluoro-alkyl-3-methylimidazolium bis(n-fluoroalkylsulfonyl)amide ionic liquids, J. Phys. Chem. B 121 (2017) 426–436.
[15] J. Huang, A. Riisager, P. Wasserscheid, R. Fehrmann, Reversible physical absorption of SO_2 by ionic liquids, Chem. Commun. (2006) 4027–4029.
[16] K. Huang, G.-N. Wang, Y. Dai, Y.-T. Wu, X.-B. Hu, Z.-B. Zhang, Dicarboxylic acid salts as task-specific ionic liquids for reversible absorption of SO_2 with a low enthalpy change, RSC Adv. 3 (2013) 16264–16269.
[17] W. Wu, B. Han, H. Gao, Z. Liu, T. Jiang, J. Huang, Desulfurization of flue gas: SO_2 absorption by an ionic liquid, Angew. Chem. Int. Ed. 43 (2004) 2415–2417.
[18] P. Wasserscheid, W. Keim, Ionic liquids — new solutions for transition metal catalysis, Angew. Chem. Int. Ed. 39 (2000) 3772–3789.
[19] C. Wang, G. Cui, X. Luo, Y. Xu, H. Li, S. Dai, Highly efficient and reversible SO_2 capture by tunable azole-based ionic liquids through multiple-site chemical absorption, J. Am. Chem. Soc. 133 (2011) 11916–11919.
[20] G. Cui, J. Zheng, X. Luo, W. Lin, F. Ding, H. Li, C. Wang, Tuning anion-functionalized ionic liquids for improved SO_2 capture, Angew. Chem. Int. Ed.

125 (2013) 10814–10818.
[21] N.V. Plechkova, K.R. Seddon, Applications of ionic liquids in the chemical industry, Chem. Soc. Rev. 37 (2008) 123–150.
[22] A. Romero, A. Santos, J. Tojo, A. Rodríguez, Toxicity and biodegradability of imidazolium ionic liquids, J. Haz. Mat. 151 (2008) 268–273.
[23] S. Tang, G.A. Baker, H. Zhao, Ether- and alcohol-functionalized task-specific ionic liquids: attractive properties and applications, Chem. Soc. Rev. 41 (2012) 4030–4066.
[24] M.J. Earle, C.M. Gordon, N.V. Plechkova, K.R. Seddon, T. Welton, Decolorization of ionic liquids for spectroscopy, Anal. Chem. 79 (2007) 758–764.
[25] E.L. Smith, A.P. Abbott, K.S. Ryder, Deep eutectic solvents (DESs) and their applications, Chem. Rev. 114 (2014) 11060–11082.
[26] Q.H. Zhang, K.D. Vigier, S. Royer, F. Jerome, Deep eutectic solvents: syntheses, properties and applications, Chem. Soc. Rev. 41 (2012) 7108–7146.
[27] D.V. Wagle, H. Zhao, G.A. Baker, Deep eutectic solvents: sustainable media for nanoscale and functional materials, Acc. Chem. Res. 47 (2014) 2299–2308.
[28] M. Francisco, A. van den Bruinhorst, M.C. Kroon, Low-transition-temperature mixtures (LTTMs): a new generation of designer solvents, Angew. Chem. Int. Ed. 52 (2013) 3074–3085.
[29] M. Hayyan, M.A. Hashim, A. Hayyan, M.A. Al-Saadi, I.M. AlNashef, M.E. Mirghani, O.K. Saheed, Are deep eutectic solvents benign or toxic? Chemosphere 90 (2013) 2193–2195.
[30] K. Radošević, M.C. Bubalo, V.G. Srček, D. Grgas, T.L. Dragičević, I.R. Redovniković, Evaluation of toxicity and biodegradability of choline chloride based deep eutectic solvents, Ecotoxicol. Environ. Saf. 112 (2015) 46–53.
[31] A. Paiva, R. Craveiro, I. Aroso, M. Martins, R.L. Reis, A.R.C. Duarte, Natural deep eutectic solvents — solvents for the 21st century, ACS Sustain. Chem. Eng. 2 (2014) 1063–1071.
[32] Y. Dai, J. van Spronsen, G.-J. Witkamp, R. Verpoorte, Y.H. Choi, Natural deep eutectic solvents as new potential media for green technology, Anal. Chim. Acta 766 (2013) 61–68.
[33] I. Zahrina, M. Nasikin, K. Mulia, Evaluation of the interaction between molecules during betaine monohydrate-organic acid deep eutectic mixture formation, J. Mol. Liq. 225 (2017) 446–450.
[34] B. Liu, F. Wei, J. Zhao, Y. Wang, Characterization of amide–thiocyanates eutectic ionic liquids and their application in SO_2 absorption, RSC Adv. 3 (2013) 2470–2476.
[35] K. Zhang, S. Ren, Y. Hou, W. Wu, Efficient absorption of SO_2 with low-partial pressures by environmentally benign functional deep eutectic solvents, J. Haz. Mat. 324 (2017) 457–463.
[36] R. Stefanovic, M. Ludwig, G.B. Webber, R. Atkin, A.J. Page, Nanostructure, hydrogen bonding and rheology in choline chloride deep eutectic solvents as a function of the hydrogen bond donor, Phys. Chem. Chem. Phys. 19 (2017) 3297–3306.
[37] D. Yang, M. Hou, H. Ning, J. Zhang, J. Ma, G. Yang, B. Han, Efficient SO_2 absorption by renewable choline chlorideglycerol deep eutectic solvents, Green Chem. 15 (2013) 2261.
[38] S. Sun, Y. Niu, Q. Xu, Z. Sun, X. Wei, Efficient SO_2 absorptions by four kinds of deep eutectic solvents based on choline chloride, Ind. Eng. Chem. Res. 54 (2015) 8019–8024.
[39] D. Deng, G. Han, Y. Jiang, Investigation of a deep eutectic solvent formed by levulinic acid with quaternary ammonium salt as an efficient SO_2 absorbent, New J. Chem. 39 (2015) 8158–8164.
[40] S.L. Perkins, P. Painter, C.M. Colina, Molecular dynamic simulations and vibrational analysis of an ionic liquid analogue, J. Phys. Chem. B 117 (2013) 10250–10260.
[41] H. Sun, Y. Li, X. Wu, G. Li, Theoretical study on the structures and properties of mixtures of urea and choline chloride, J. Mol. Model 19 (2013) 2433–2441.
[42] G. García, M. Atilhan, S. Aparicio, An approach for the rationalization of melting temperature for deep eutectic solvents from DFT, Chem. Phys. Lett. 634 (2015) 151–155.
[43] S. Zhu, H. Li, W. Zhu, W. Jiang, C. Wang, P. Wu, Q. Zhang, H. Li, Vibrational analysis and formation mechanism of typical deep eutectic solvents: an experimental and theoretical study, J. Mol. Graph. Modell. 68 (2016) 158–175.
[44] D.V. Wagle, C.A. Deakyne, G.A. Baker, Quantum chemical insight into the interactions and thermodynamics present in choline chloride based deep eutectic solvents, J. Phys. Chem. B 120 (2016) 6739–6746.
[45] C.R. Ashworth, R.P. Matthews, T. Welton, P.A. Hunt, Doubly ionic hydrogen bond interactions within the choline chloride-urea deep eutectic solvent, Phys. Chem. Chem. Phys. 18 (2016) 18145–18160.
[46] S. Zahn, B. Kirchner, D. Mollenhauer, Charge spreading in deep eutectic solvents, ChemPhysChem 17 (21) (2016) 3354–3358.
[47] S. Zahn, Deep eutectic solvents: *Similia similibus solvuntur*? Phys. Chem. Chem. Phys. 19 (2017) 4041–4047.
[48] H. Li, Y. Chang, W. Zhu, C. Wang, C. Wang, S. Yin, M. Zhang, H. Li, Theoretical evidence of charge transfer interaction between SO_2 and deep eutectic solvents formed by choline chloride and glycerol, Phys. Chem. Chem. Phys. 17 (2015) 28729–28742.
[49] D.S. Firaha, M. Kavalchuk, B. Kirchner, SO_2 solvation in the 1-ethyl-3-methylimidazolium thiocyanate ionic liquid by incorporation into the extended cation–anion network, J. Solut. Chem. 44 (2015) 838–849.
[50] B. Kirchner, P.J. di Dio, J. Hutter, Real-world predictions from ab initio molecular dynamics simulations, in: B. Kirchner, J. Vrabec (Eds.), Multiscale Molecular Methods in Applied Chemistry, Vol. 307 of Topics in Current Chemistry, Springer Berlin Heidelberg, 2012, pp. 109–153.
[51] O. Borodin, Polarizable force field development and molecular dynamics simulations of ionic liquids, J. Phys. Chem. B 113 (2009) 11463–11478.
[52] C. Schröder, Comparing reduced partial charge models with polarizable simulations of ionic liquids, Phys. Chem. Chem. Phys. 14 (2012) 3089–3102.
[53] A. Dequidt, J. Devémy, A.A.H. Pádua, Thermalized drude oscillators with the lammps molecular dynamics simulator, J. Chem. Inf. Model 56 (2016) 260–268.
[54] M. Salanne, L.J.A. Siqueira, A.P. Seitsonen, P.A. Madden, B. Kirchner, From molten salts to room temperature ionic liquids: simulation studies on chloroaluminate systems, Faraday Discuss. 154 (2012) 171–188.
[55] H. Weber, M. Salanne, B. Kirchner, Toward an accurate modeling of ionic liquid–TiO_2 interfaces, J. Phys. Chem. C 119 (2015) 25260–25267.
[56] S. Plimpton, Fast parallel algorithms for short-range molecular dynamics, J. Comp. Phys. 117 (1995) 1–19.
[57] K. Shahbaz, S. Baroutian, F. Mjalli, M. Hashim, I. AlNashef, Densities of ammonium and phosphonium based deep eutectic solvents: prediction using artificial intelligence and group contribution techniques, Thermochim. Acta 527 (2012) 59–66.
[58] CP2K Open Source Molecular Dynamics Home Page. Oficial Webpage: http://www.cp2k.org (Accessed 01 March 2013).
[59] J. VandeVondele, M. Krack, F. Mohamed, M. Parrinello, T. Chassaing, J. Hutter, Quickstep: fast and accurate density functional calculations using a mixed gaussian and plane waves approach, Comput. Phys. Commun. 167 (2005) 103–128.
[60] J. VandeVondele, J. Hutter, Gaussian basis sets for accurate calculations on molecular systems in gas and condensed phases, J. Chem. Phys. 127 (2007) 114105.
[61] A.D. Becke, Density-functional exchange-energy approximation with correct asymptotic behavior, Phys. Rev. A 38 (1988) 3098–3100.
[62] C. Lee, W. Yang, R.G. Parr, Development of the colle-salvetti correlation-energy formula into a functional of the electron density, Phys. Rev. B 37 (1988) 785–789.
[63] S. Goedecker, M. Teter, J. Hutter, Separable dual-space gaussian pseudopotentials, Phys. Rev. B 54 (1996) 1703–1710.
[64] C. Hartwigsen, S. Goedecker, J. Hutter, Relativistic separable dual-space gaussian Pseudopotentials from H to Rn, Phys. Rev. B 58 (1998) 3641–3662.
[65] M. Krack, Pseudopotentials for h to kr optimized for gradient-corrected exchange-correlation functionals, Theor. Chem. Acc. 114 (2005) 145–152.
[66] S. Grimme, J. Antony, S. Ehrlich, H. Krieg, A consistent and accurate ab initio parametrization of density functional dispersion correction (DFT-D) for the 94 elements H-Pu, J. Chem. Phys. 132 (2010) 154104.
[67] S. Grimme, S. Ehrlich, L. Goerigk, Effect of the damping function in dispersion corrected density functional theory, J. Comp. Chem. 32 (2011) 1456–1465.
[68] S. Zahn, G. Bruns, J. Thar, B. Kirchner, What keeps ionic liquids in flow? Phys. Chem. Chem. Phys. 10 (2008) 6921–6924.
[69] S. Grimme, W. Hujo, B. Kirchner, Performance of dispersion-corrected density functional theory for the interactions in ionic liquids, Phys. Chem. Chem. Phys. 14 (2012) 4875–4883.
[70] F. Malberg, A.S. Pensado, B. Kirchner, The bulk and the gas phase of 1-ethyl-3-methylimidazolium ethylsulfate: dispersion interaction makes the difference, Phys. Chem. Chem. Phys. 14 (2012) 12079–12082.
[71] A.S. Pensado, M. Brehm, J. Thar, A.P. Seitsonen, B. Kirchner, Effect of dispersion on the structure and dynamics of the ionic liquid 1-ethyl-3-methylimidazolium thiocyanate, ChemPhysChem 13 (7) (2012) 1845–1853.
[72] S. Zahn, B. Kirchner, Uncovering molecular secrets of ionic liquids, in: chemical modelling: applications and theory volume 9, R. Soc. Chem. 9 (2012) 1–24.
[73] D.S. Firaha, M. Thomas, O. Hollóczki, M. Korth, B. Kirchner, Can dispersion corrections annihilate the dispersion-driven nano-aggregation of non-polar groups? An ab initio molecular dynamics study of ionic liquid systems, J. Chem. Phys. 145 (2016) 204502.
[74] E.I. Izgorodina, U.L. Bernard, D.R. MacFarlane, Ion-pair binding energies of ionic liquids: can DFT compete with ab initio-based methods? J. Phys. Chem. A 113 (2009) 7064–7072.
[75] E.I. Izgorodina, Z.L. Seeger, D.L. Scarborough, S.Y. Tan, Quantum chemical methods for the prediction of energetic, physical, and spectroscopic properties of ionic liquids, Chem. Rev. (2017). http://dx.doi.org/10.1021/acs.chemrev.6b00528.
[76] A. Bankura, A. Karmakar, V. Carnevale, A. Chandra, M.L. Klein, Structure, dynamics, and spectral diffusion of water from first-principles molecular dynamics, J. Phys. Chem. C 118 (2014) 29401–29411.
[77] S. Nosé, A unified formulation of the constant temperature molecular-dynamics methods, J. Chem. Phys. 81 (1984) 511–519.
[78] W.G. Hoover, Canonical dynamics - equilibrium phase-space distributions, Phys. Rev. A 31 (1985) 1695–1697.
[79] M. Brehm, B. Kirchner, Travis - a free analyzer and visualizer for monte carlo and molecular dynamics trajectories, J. Chem. Inf. Model 51 (8) (2011) 2007–2023.
[80] Gnuplot. Home Page: http://www.gnuplot.info (Accessed 10 October 2015).
[81] Xmgrace. Home Page: http://plasma-gate.weizmann.ac.il/Grace/ (Accessed 15 October 2015).
[82] M. Thomas, M. Brehm, B. Kirchner, Voronoi dipole moments for the simulation of bulk phase vibrational spectra, Phys. Chem. Chem. Phys. 17 (2015) 3207–3213.

[83] M. Brehm, H. Weber, M. Thomas, O. Hollóczki, B. Kirchner, Domain analysis in nanostructured liquids: a post-molecular dynamics study at the example of ionic liquids, ChemPhysChem 16 (15) (2015) 3271–3277.
[84] R. Ahlrichs, M. Bär, M. Häser, H. Horn, C. Kölmel, Electronic structure calculations on workstation computers: the program system turbomole, Chem. Phys. Lett. 162 (1989) 165–169.
[85] M.C.C. Ribeiro, Molecular dynamics simulation of liquid sulfur dioxide, J. Phys. Chem. B 110 (2006) 8789–8797.
[86] O. Hollóczki, M. Macchiagodena, H. Weber, M. Thomas, M. Brehm, A. Stark, O. Russina, A. Triolo, B. Kirchner, Triphilic ionic-liquid mixtures: fluorinated and non-fluorinated aprotic ionic-liquid mixtures, ChemPhysChem 16 (2015) 3325–3333.